

INTERACTION OF LASER RADIATION WITH MATTER. LASER PLASMA

PACS numbers: 33.80.Wr; 42.70.Mp; 42.70.Nq
DOI: 10.1070/QE2012v042n07ABEH014846

Interband two-photon absorption in strontium barium niobate crystals

P.G. Zverev, L.I. Ivleva, A.Ya. Karasik, V.I. Lukanin, D.S. Chunaev

Abstract. **Interband two-photon absorption in photorefractive strontium barium niobate crystals $Sr_xBa_{1-x}Nb_2O_6$ (x = 0.61, 0.75), both pure and doped with Ni and La ions, is studied under excitation by trains of 523.5-nm picosecond laser pulses. The two-photon absorption coefficients are found to vary from 0.17 to 0.31 cm GW^{-1} depending on the azimuth of the linear polarisation of the pump radiation and on the chemical composition of samples. The dependences of the transmission of crystals on the pump radiation intensity show a hysteresis related to induced one-photon absorption from excited levels.**

Keywords: *strontium barium niobate crystals, two-photon absorption, interband absorption, photorefractive crystal.*

1. Introduction

The ferroelectric strontium barium niobate (SBN) crystals were synthesised for the first time in the 60s of the previous century. The SBN solid solutions belong to the class of relaxor ferroelectrics and have unique photorefractive, electrooptic, nonlinear optical, and dielectric characteristics [1]. Owing to the extremely high dielectric constant and pyro-, piezo-, and electrooptic coefficients, these materials are widely used both in ordinary structures and in films and waveguides [2–4]. The properties of $Sr_xBa_{1-x}Nb_2O_6$ crystals are determined both by their composition (x may vary from 0.20 to 0.85) and by the content of specially introduces impurities. Doped SBN crystals (with Ce, Cr, Co impurities) are very promising materials for dynamic holography, in particular, for phase conjugation and optical memory, as well as for efficient control of the space–time parameters of optical radiation and for fabrication of electrooptic modulators and switches [5–8].

In addition to practical applications, SBN crystals are of interest for fundamental studies and can be considered as model objects for investigation of systems with disordered structures [9, 10]. The introduction of impurities changes the optical transparency of crystals and enhances their photorefractive and dielectric properties. The possibility of using SBN crystals as optical memory cells or for recording long-lived holograms relates, in particular, to the nonlinear process of four-wave mixing. In addition to the unique photorefractive properties, the SBN crystals exhibit strong nonlinear optical properties, for example, the authors of [11] observed stimulated Raman scattering due to symmetric high-frequency vibrations of the $(NbO_3)^-$ anionic complex. However, almost no data are available on the constants of nonlinear processes determining the intensity of these vibrations.

In this work, we study the nonlinear process of interband two-photon absorption (TPA) in SBN crystals and measure the TPA coefficients. The processes of generation and decay of electronic excitations upon two- and one-photon absorption (OPA) in inorganic and organic media (in particular, in oxide and fluoride materials and semiconductors) under nano-, pico-, and femtosecond laser excitation attract great attention, which is evidenced by a large number of publications (see, for example, [12–15]).

The TPA provides additional possibilities for spectroscopy, especially for excitation of electronic states in the conduction band, where materials are almost nontransparent, whereas the OPA allows one to perform investigations mainly by the methods of luminescence spectroscopy. In the case of interband TPA, in contrast to OPA, one obtains uniform bulk excitation of a medium and can get rid of nonradiative near-surface losses, which appear in the case of OPA and depend on the material surface quality [16]. The difference in the selection rules for the OPA and TPA electronic transitions also extends the possibilities of investigations. The measurement of TPA coefficients for different media is a separate problem. These coefficients are unknown for a great number of materials widely used in both nonlinear optics and detectors of ionising radiation. The TPA can be used to control the energy, temporal, spectral, and spatial parameters of laser radiation, for example, to control the power and duration of laser pulses [13]. The TPA method makes it possible to improve the spatial resolution in laser microstructuring of materials and in microscopy [17].

Previously, we studied the TPA in tungstate and molybdate oxide crystals, which are of special interest for creating ionising radiation detectors [16] and SRS frequency converters [18]. We developed a TPA method with picosecond resolution upon excitation by a train of laser pulses with a smoothly and continuously changing intensity. This allowed us to obtain new information about the processes of generation and relaxation of electronic excitations and to measure the TPA coefficients in oxide crystals, as well as to compare the TPA and SRS gain coefficients and to evaluate the competition of these nonlinear processes related to the cubic nonlinear susceptibility [19, 20].

P.G. Zverev, L.I. Ivleva, A.Ya. Karasik, V.I. Lukanin, D.S. Chunaev
A.M. Prokhorov General Physics Institute, Russian Academy of Sciences, ul. Vavilova 38, 119991 Moscow, Russia;
e-mail: zverev@lst.gpi.ru

Received 6 March 2012; revision received 25 April 2012
Kvantovaya Elektronika **42** (7) 595–599 (2012)
Translated by M.N. Basieva

The aim of this work is to study the two-photon absorption in SBN crystals under excitation by picosecond laser pulses with a wavelength of 523.5 nm.

2. Objects of investigation

The samples of crystals under study were made of nominally pure SBN-61 (x = 0.61) and SBN-75 (x = 0.75) crystals, as well as of SBN-61 crystals doped with Ni (0.05 wt % of Ni_2O_3), La (0.5 wt % of La_2O_3), and Co (0.05 wt % of Co_3O_4), which were grown at the A.M. Prokhorov General Physics Institute, Russian Academy of Sciences, by the modified Stepanov method [21]. Dopants were introduced into the charge in the form of corresponding oxides before the crystal growth process. At small concentrations of dopants, the effective distribution coefficient is close to unity, because of which the crystals were characterised by the concentrations of impurities introduced into the charge. The experimental samples had a rectangular shape with a cross section of 6×8 mm and a length of 8–11 mm; the crystallographic C_4 axis being perpendicular to the beam propagation direction. The samples under study belong to the class of relaxor ferroelectrics, which are characterised by the existence of 180-degree domains and by a smeared phase transition. The ferroelectric-to-paraelectric phase transition for these crystals occurs at temperatures from 60 to 80 °C depending on the crystal composition [22, 23]. Our experiments with SBN crystals were performed at room temperature. We used experimental samples without preliminary poling.

3. Experimental results and discussion

The short-wavelength transmission edge of SBN crystals lies in the region of 380–530 nm depending on the crystal type and concentration of dopants (Fig. 1). In the near UV region, the absorption spectra of pure SBN-61 and SBN-75 crystals and of doped SBN-61(La) crystals coincide with each other [Fig. 1., curve (*1*)]. Doping with Ni and Co creates additional energy levels, which enhances the photorefractive properties of crystals [21] and leads to a shift of the absorption edge to longer wavelengths [Fig. 1, curves (*2*) and (*3*)].

The experimental setup for studying TPA is described in detail in [20]. The crystals were excited by the second harmonic (523.5 nm) of a passively mode-locked Nd : YAG laser. The excitation photon energy ($h\nu$ = 2.36 eV) falls into the transparency region for all the studied crystals except for SBN-61(Co). The energy of two excitation photons, which is equal to 4.72 eV, falls into the conduction band of the crystals ($h\nu < E_g < 2h\nu$). The pump laser operated in the single transverse TEM_{00} mode. It emitted a train of polarised transform-limited pulses with a duration of 20 ps, the total train energy being up to 3 mJ. The train duration was about 100 ns and the repetition rate was up to 10 Hz. The laser beam was focused into the sample by a lens with f = 112 nm. The temporal structure of the passed radiation was recorded by a fast germanium photodiode and analysed by a Tektronix DPO 4104 digital oscilloscope with a bandwidth of 1 GHz. The spatial profile of the pump radiation was recorded using a silicon CCD camera and was found to be close to Gaussian. The energy of individual picosecond pulses was determined by measuring the total train energy and the amplitudes of individual pulses on the oscillogram. The used method based on the measurement of the crystal transmission under single excitation by a train of laser pulses allows one to increase the measurement accuracy compared to the case of multiple excitation with accumulation and averaging of signals [12, 19, 20].

Figure 2 shows the synchronised oscillograms of pulse trains at the entrance (I_0) and exit (I) of an SBN-75 crystal. One can see that the shape of the envelope of the pulse train passed through the sample is changed, namely, the train maximum shifts to the beginning of the train. This is explained by a decrease in the pulse intensity due to TPA, as well as by induced OPA [19]. Note that, in the SBN-61(Co) crystal, in which the excitation wavelength of 523.5 nm corresponds to OPA [Fig. 1, curve (*3*)], TPA was not observed.

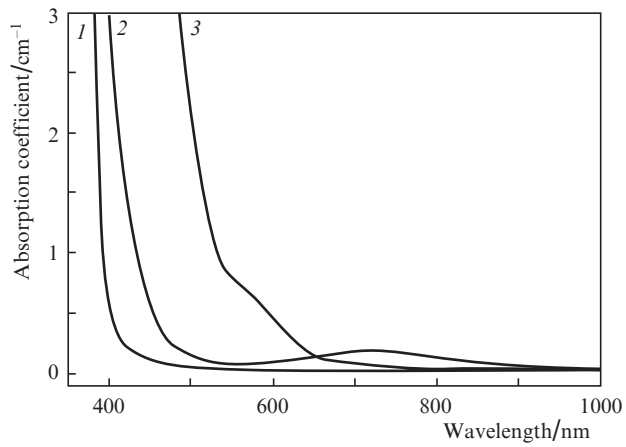

Figure 1. Absorption spectra of SBN-75, SBN-61, and SBN-61(La) crystals (*1*), as well as of SBN-61(Ni) (*2*) and SBN-61(Co) crystals (*3*).

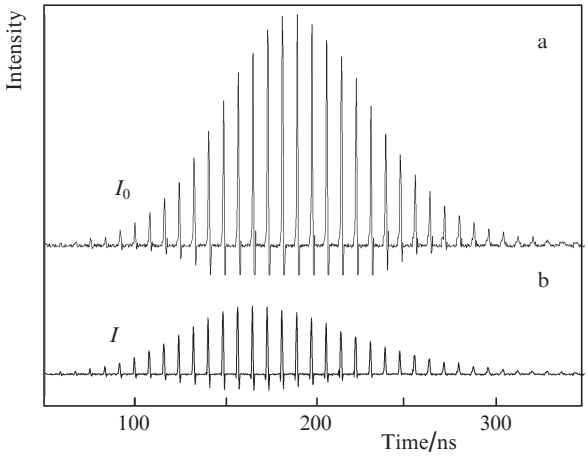

Figure 2. Oscillograms of the trains of laser pulses at the entrance I_0 (a) and exit I (b) of an SBN-75 crystal 11 mm long for polarisation $\boldsymbol{E} \| C_4$.

Figure 3 presents the dependences of the intensity I of individual picosecond pulses at the exit of the crystal on the incident intensity I_0 for SBN-75 and SBN-61(La) crystals. The experimental points are obtained by measuring the amplitudes on oscillograms of corresponding picosecond pulses at the entrance and exit of the crystal. The arrows near the curves in Fig. 3 denote the progression of pulses in the train. The dashed line shows the linear intensity dependence that takes into account the Fresnel losses

in samples. It is seen that the consistent increase in the pulse intensity I_0 of the first half of the train leads to an increase in the output intensity I. The experimental dependence gradually deviates from the linear law due to the TPA. After passing the maximum, the intensity I_0 of incident pulses of the second part of the train decreases and the output intensity I also continuously decreases. The energy dependence exhibits a characteristic hysteresis, and one can see that the hysteresis loop width depends on the crystal orientation. In the case when the linear polarisation of the pump radiation is directed parallel to the C_4 crystallographic axis, the hysteresis is more pronounced than in the case of the orthogonally polarised radiation. An increase in the incident pulse intensity above 10 GW cm^{-2} can cause optical breakdown of samples.

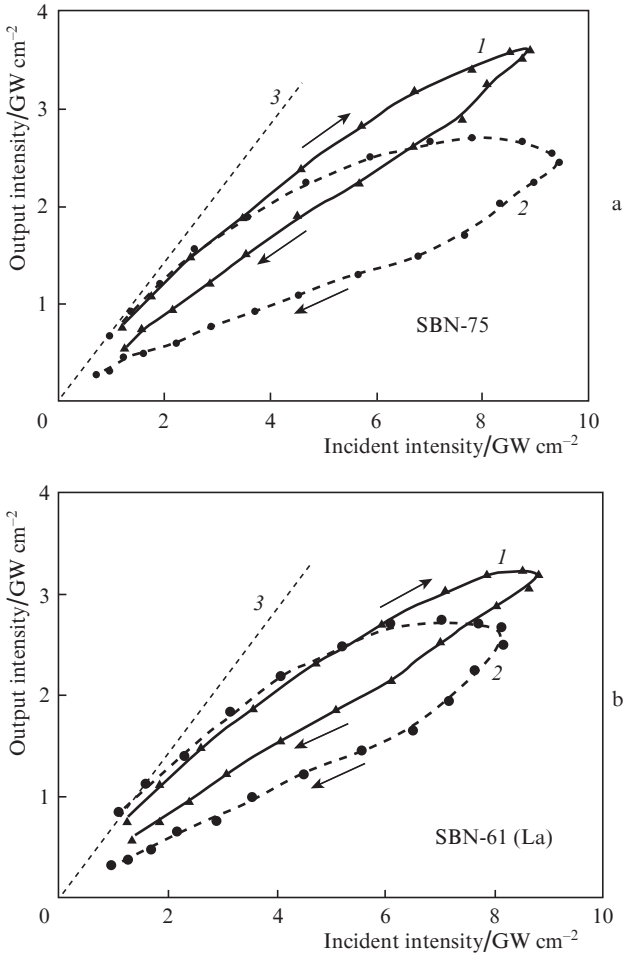

Figure 3. Dependences of the output radiation intensity I on the incident radiation intensity I_0 for an SBN-75 crystal 11 mm long (a) and an SBN-61(La) crystal 9.5 mm long (b) in the case of $\boldsymbol{E}\perp C_4$ (*1*) and $\boldsymbol{E}\parallel C_4$ (*2*) polarisations, as well as calculated linear dependence taking into account the Fresnel losses (*3*).

We relate the appearance of hysteresis to the one-photon absorption from the excited level, induced by the interband TPA. In [19], we showed that the absorption of two 523.5-nm photons in tungstate and molybdate crystals is accompanied by the absorption of a third (probe) 523.5-nm photon, which increases the excited state population and reflects the induced OPA kinetics.

Figure 4 shows the dependences of the reciprocal transmission $1/T = I_0/I$ for an SBN-61(La) crystal on the incident radiation intensity I_0 for polarisations $\boldsymbol{E}\perp C_4$ (a) and $\boldsymbol{E}\parallel C_4$ (b). The experimental points were obtained by dividing the amplitudes of pulses in the first oscillogram by the corresponding amplitudes in the second oscillogram (Fig. 2). It is seen that the value $1/T$ linearly increases with increasing the incident intensity I_0 to some level. This testifies to a gradual increase in the sample absorption due to the TPA. At higher I_0, all the measured dependences deviate from linear as a result of an increase in the time-dependent induced OPA coefficient $\alpha(t)$. The absorption coefficient in this case can be written in the form $k = \beta I + \alpha(t)$. As was show in [19] for tungstate and molybdate crystals, the induced absorption dynamics in a wide time range (from nanoseconds to hundreds of milliseconds) can be different. However, at the initial stage, before the appearance of a considerable induced OPA, the dependences of the reciprocal transmission $1/T$ on the pump radiation intensity are linear (Fig. 4). In this case, the TPA coefficient can be determined from the slope of these linear dependences. The extrapolation of the linear dependence to its intersection with the ordinate axis allows one to determine the initial transmission of the crystal.

Previously, we measured the wavelength dependence of the refractive index for an SBN-61 crystal and found n_o =

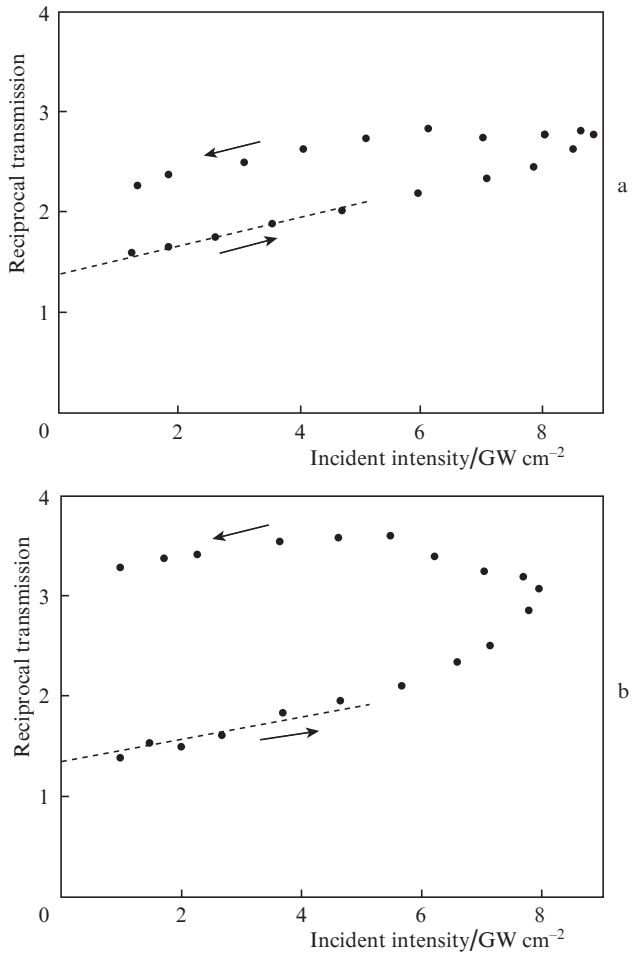

Figure 4. Dependence of the reciprocal transmission $1/T$ on the incident intensity I_0 for an SBN-61(La) crystal 10 mm long and polarisations $\boldsymbol{E}\perp C_4$ (a) and $\boldsymbol{E}\parallel C_4$(b).

2.364 and $n_e = 2.327$ for $\lambda = 523.5$ nm. The refractive index remained the same within the second decimal with changing the crystal composition and doping. The Fresnel losses for one surface are $T_{Fr} = 4n/(n+1)^2$ and, hence, taking into account reflection from two faces, the sample transmission is 0.698 % and 0.707 %, respectively. Figure 4 shows that the initial reciprocal transmission for both polarisations of the pump radiation is $1/T_0 = 1.4$, which corresponds to the losses related to the Fresnel reflection and points to a good optical quality of the studied crystals.

The TPA coefficients β were calculated from the initial linear part of the experimental dependence of the reciprocal transmission $1/T$ on the incident radiation intensity I_0 (dashed line) [13, 20]. The TPA coefficient is determined as

$$\beta = \frac{bT_0}{L}, \tag{1}$$

where $b = \Delta(T^{-1})/\Delta I_0$ is the slope of the linear dependence; T_0 is the initial transmission of the sample; and $L \approx 10$ mm is the nonlinear interaction length [20], which is close to the real length of the studied samples. The measured TPA coefficients β of the studied crystals for different polarisations of the pump radiation are listed in Table 1. The error in the determination of β was ~20% [20]. One can see that the value of β varies depending on the sample composition and dopants. The change of the orientation of the pump radiation polarisation with respect to the crystallographic axis of samples from $\boldsymbol{E} \| C_4$ to $\boldsymbol{E} \perp C_4$ leads to a decrease in the β coefficient in all the crystals. Note that a similar effect of the polarisation anisotropy of TPA is also typical for organic materials [12].

Due to a strongly incongruent composition, the SBN-75 crystals have the most disordered structure, because of which, in the case of the optimal orientation, they have the most pronounced electrooptical properties among all the SBN crystals. Table 1 demonstrates that the SBN-75 crystal also has the highest TPA coefficient ($\beta = 0.31$ cm GW^{-1}), which decreases to 0.18 cm GW^{-1} for the orthogonal pump polarisation. The SBN-61 crystal had a congruent composition and is characterised by a relatively weak anisotropy of nonlinear optical properties. Doping of these crystals with rare-earth ions and transition metals leads to an enhancement of their relaxor characteristics, to a decrease in the Curie temperature, and to an increase in the ferroelectric, nonlinear optical, and photorefractive parameters [21], which causes a slight increase in the TPA coefficient in the SBN-61(La) crystal. The low TPA coefficient in the SBN-61(Ni) crystal can be related to the observed anomalous decrease in its dielectric constants as a result of doping by Ni with concentrations exceeding 0.5 wt % [24].

The found TPA coefficients allow us to compare the experimental maximum output intensity (Fig. 3) with the theoretical estimate of the TPA-limited intensity I_{max} [17],

Table 1. TPA coefficients β of SBN crystals measured for two polarisations of pump radiation.

Crystal	β/cm GW^{-1}	
	$\boldsymbol{E} \perp C_4$	$\boldsymbol{E} \| C_4$
SBN-61	0.23	0.27
SBN-75	0.18	0.31
SBN-61(Ni)	0.16	0.17
SBN-61(La)	0.25	0.29

$$I_{max} = 1/\beta L. \tag{2}$$

For an SBN-75 sample 11 mm long, the formula (2) yields $I_{max} = 5.0$ and 2.9 GW cm^{-2} for $\boldsymbol{E} \perp C_4$ and $\boldsymbol{E} \| C_4$, respectively. The corresponding experimental values of I_{max} are 3.5 and 2.7 GW cm^{-2} (Fig. 3a). One can see a good agreement between theory and experiment for $\boldsymbol{E} \| C_4$, which indicates that we reached a regime in which the radiation intensity is limited by TPA. In the case of the orthogonal polarisation ($\boldsymbol{E} \perp C_4$), for which β is almost two times smaller, the limiting regime is not yet reached. For the SBN-61(La) crystal 9.5 mm long, the calculated I_{max} is 4.2 and 3.6 GW cm^{-2} for polarisations $\boldsymbol{E} \perp C_4$ and $\boldsymbol{E} \| C_4$, while the corresponding experimental values are 3.2 and 2.8 GW cm^{-2} (Fig. 3b), which means that the regime is close to limiting.

In [20], we determined the TPA coefficients for molybdate and tungstate crystals. The minimum TPA coefficients β for SBN crystals are 0.16–0.18 cm GW^{-1} and are comparable with 0.14 cm GW^{-1} for $CaMoO_4$ crystals. At the same time, the maximum TPA coefficients in SBN crystals are considerably smaller than in $PbMoO_4$ and $PbWO_4$ crystals, which have $\beta = 2.4$ and 2.0 cm GW^{-1}, respectively.

The relatively low TPA coefficients and, hence, low imaginary parts of the cubic nonlinear susceptibility in SBN crystals are responsible for the low SRS gains, which is confirmed by the results of [11]. Note that we did not observed SRS in our experiments with SBN crystals excited by 523.5-nm radiation.

4. Conclusions

In this work, the interband TPA in pure and La- and Ni-doped SBN crystals upon 532.5-nm picosecond excitation is studied for the first time. The TPA coefficients are measured to vary from 0.18 to 0.31 cm GW^{-1} depending on the pump radiation polarisation and the crystal composition. It is shown that the TPA leads to induced one-photon absorption from excited states.

The TPA process limits the laser radiation intensity, which can be used for stabilisation and limiting of radiation intensity in optical devices. The TPA may compete with other nonlinear processes related to cubic nonlinearity, for example, with SRS or four-wave mixing. This circumstance must be taken into account when developing new nonlinear optical devices based on photorefractive strontium barium niobate crystals.

Acknowledgements. This work was supported by the Ministry of Education and Science of the Russian Federation (State Contract No. 16.513.12.3019) and by the Russian Foundation for Basic Research (Grant No. 10-02-00254a).

References

1. Prokhorov A.M., Kuz'minov Yu.S. *Ferroelectric Crystals for Laser Radiation Control* (Bristol–Philadelphia –New-York: Adam Hilger, 1990).
2. Trivedi D., Tayebati P., Tabat M. *Appl. Phys. Lett.*, **68**, 3227 (1996).
3. Marx J.M., Eknoyan O., Naylor H.F., Tang Z., Neurgaonkar R.R. *Appl. Phys. Lett.*, **67**, 1381 (1995).
4. Usievich B.A., Nurligareev D.Kh., Sychugov V.A., Ivleva L.I., Lykov P.A., Bogodaev N.V. *Kvantovaya Elektron.*, **40** (5), 437 (2010) [*Quantum Electron.*, **40** (5), 437 (2010)].
5. Isakov D.V., Belsley M.S., Volk T.R., Ivleva L.I. *Appl. Phys. Lett.*, **92**, 032904 (2008).

6. Bogodaev N.V., Ivleva L.I., Korshunov A.S., Polozkov N.M., Shkunov V.V. *J. Opt. Soc. Am. B*, **10**, 2287 (1993).
7. Bogodaev N.V., Ivleva L.I., Korshunov A.S., Mamaev A.V., Polozkov N.M., Zozulya A.A. *J. Opt. Soc. Am. B*, **10**, 1054 (1993).
8. Berezhnoi A.A. *Opt. Zh.*, **66**, 3 (1999).
9. Granzow T., Woike Th., Imlau M., Kleemann W. *Phys. Rev. Lett*., **89**, 127601 (2002).
10. Kleemann W., Dec J., Blinc R., Zalar B., Pankrath R. *Europhys. Lett*., **57**, 14 (2002).
11. Basiev T.T., Doroshenko M.E., Ivleva L.I., Smetanin S.N., Jelinek M., Kubecek V., Jelinkova H. *Laser Phys. Lett*., **9,** 519 (2012).
12. Rumi M., Perry W. *Adv. Opt. Photon*., **2**, 451 (2010).
13. Arsen'ev V.V., Dneprovskii V.S., Klyshko D.N., Penin A.N. *Zh. Eksp. Teor. Fiz*., **56**, 761 (1969) [*JETP*, **29**, 413 (1969)].
14. Bezel I.V., Matveets Yu.A., Stepanov A.G., Chekalin S.V., Yartsev A.P. *Pis'ma Zh. Eksp. Teor. Fiz*., **59**, 376 (1994) [*JETP Lett*., **59**, 403 (1994)].
15. Artem'ev M.Yu., Nesterov V.M., Sergeev A.P., Sergeev P.B. *Kvantovaya Elektron.*, **34** (2), 147 (2004) [*Quantum Electron*., **34** (2), 147 (2004)].
16. Groenik J.A., Blasse G. *J. Solid State Chem*., **32**, 9 (1980).
17. Korte F., Serbin J., Koch J., Egbert A., Fallnich C., Ostendorf A., Chichkov B.N. *Appl. Phys. A*, **77**, 229 (2003).
18. Basiev T.T., Zverev P.G., Karasik A.Ya., Osiko V.V., Sobol A.A., Chunaev D.S. *Zh. Eksp. Teor. Fiz*., **126**, 1073 (2004) [*JETP*, **99**, 934 (2004)].
19. Lukanin V.I., Chunaev D.S., Karasik A.Ya. *Pis'ma Zh. Eksp. Teor. Fiz*., **91**, 615 (2010) [*JETP Lett*., **91**, 548 (2010)].
20. Lukanin V.I., Chunaev D.S., Karasik A.Ya. *Zh. Eksp. Teor. Fiz*., **140**, 472 (2011) [*JETP*, **113**, 412 (2011)].
21. Ivleva L.I. *Izv. RAN. Ser. Fiz*., **73**, 1413 (2009) [*Bull. Russ. Acad. Sci., Ser. Fiz*., **73**, 1413 (2009)].
22. Volk T.P., Salobutin V.Yu., Ivleva L.I., Polozkov N.M., Pankrath R., Woehlecke, M. *Fiz. Tverdogo Tela,* **42**, 2066 (2000).
23. Ivleva L.I., Bogodaev N.V., Lykov P.A., Osiko V.V., Polozkov N.M., Volk T.R. *Laser Phys*., **13**, 251 (2003).
24. Matyjasek K., Wolska K., Kaczmarek S.M., Subocz J., Ivleva L. *Appl. Phys. B*, **106**, 143 (2012).